Electrostatic supersolitons in three-species plasmas

Frank Verheest' , Manfred A. Hellberg' , and Ioannis Kourakis'

Citation: Physics of Plasmas **20**, 012302 (2013); doi: 10.1063/1.4775085
View online: http://dx.doi.org/10.1063/1.4775085
View Table of Contents: http://aip.scitation.org/toc/php/20/1
Published by the American Institute of Physics

Electrostatic supersolitons in three-species plasmas

Frank Verheest,[1,2,a)] Manfred A. Hellberg,[2,b)] and Ioannis Kourakis[3,c)]
[1]*Sterrenkundig Observatorium, Universiteit Gent, Krijgslaan 281, B–9000 Gent, Belgium*
[2]*School of Chemistry and Physics, University of KwaZulu-Natal, Durban 4000, South Africa*
[3]*Department of Physics and Astronomy, Centre for Plasma Physics, Queen's University Belfast, BT7 1NN Northern Ireland, United Kingdom*

(Received 13 December 2012; accepted 21 December 2012; published online 10 January 2013)

Superficially, electrostatic potential profiles of supersolitons look like those of traditional solitons. However, their electric field profiles are markedly different, having additional extrema on the wings of the standard bipolar structure. This new concept was recently pointed out in the literature for a plasma model with five species. Here, it is shown that electrostatic supersolitons are not an artefact of exotic, complicated plasma models, but can exist even in three-species plasmas and are likely to occur in space plasmas. Further, a methodology is given to delineate their existence domains in a systematic fashion by determining the specific limiting factors. © *2013 American Institute of Physics*. [http://dx.doi.org/10.1063/1.4775085]

I. INTRODUCTION AND MOTIVATION

Nonlinear solitary waves (often called solitons even if the required mathematical conditions are not met) occur in various physical contexts.[1] Their first (historical) mathematical description showed that weakly nonlinear solitary waves on shallow water preserved their shape through a balance between nonlinear steepening and dispersion, and even maintained their shape after mutual interactions (collisions),[2] earning them later the name of "solitons,"[3] to emphasize their particle-like character.

Soliton research in plasmas is an old topic.[4] Our work will focus on fully nonlinear solitary electrostatic structures in multifluid plasmas. Adopting a (by now widely used) stationary-profile traveling coordinate transformation, fluid plasma models were originally associated with fully nonlinear electrostatic, acoustic-type solitons via Sagdeev's seminal work.[5] This reduces the fluid equations, together with Poisson's equation, to a pseudomechanical energy-balance equation, involving a pseudopotential $S(\varphi)$, where φ is the electric potential. An equivalent fluid dynamical analysis has also been used.[6,7] Integration then leads to hump or dip soliton profiles for the electric potential, and thus to bipolar forms for the electric field, E. One may also obtain a kink in φ, known as a double layer. The soliton/double layer model has been valuable when interpreting observations in both space[8–12] and the laboratory.[13–15]

This framework has recently been extended to embrace a new development, namely, the concept of electrostatic *super solitary waves* (or *supersolitons* for short). Considering five-species plasmas, Dubinov and Kolotkov[16,17] introduced the nomenclature and presented examples of such structures. Although, superficially, the potential profiles of supersolitons might look like traditional solitons, there is a marked difference when their electric fields are plotted. The bipolar structures calculated in most standard scenarios and reported in numerous space environments[18,19] are now seen to be "embroidered" with local extrema ("wiggles"). This is illustrated in Fig. 1 with an example of a standard soliton compared to a supersoliton, and their associated electric fields, more details of which will be given below. The presence of subsidiary maxima on the wings of the bipolar structure provides a signature that should enable supersolitons to be identified in observations, depending on the level of resolution obtainable. Citing Ref. 20, Dubinov and Kolotkov[16] suggested that a plasma of at least four species was required to support pseudopotentials with the necessary wiggles to yield supersolitons.

The present paper, first, provides evidence that such supersolitons can occur in the less complicated scenario of three-species plasmas. Second, we present a methodology to delineate the existence domain of supersolitons in compositional parameter and Mach number space for a typical case, and draw attention to the limiting factors.

Supersolitons have a number of characteristics. As shown below, their existence requires the presence, in the

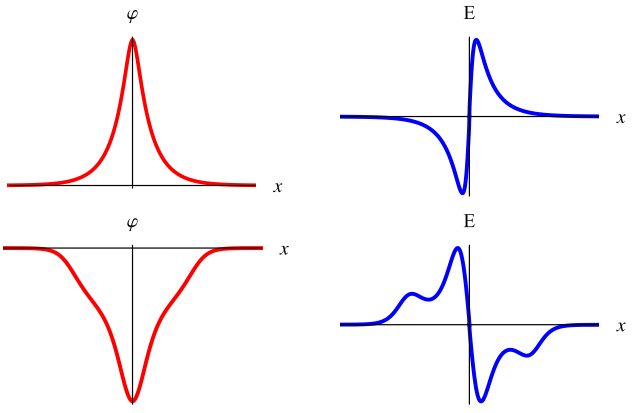

FIG. 1. *Upper panels:* Example of a standard positive soliton and its associated electric field. *Lower panels:* A negative supersoliton and its associated electric field.

[a)]email: frank.verheest@ugent.be
[b)]email: hellberg@ukzn.ac.za
[c)]email: i.kourakis@qub.ac.uk

Sagdeev pseudopotential well, $S(\varphi)$, of at least three local extrema between $\varphi = 0$ and the soliton amplitude, φ_m.[16] Pseudopotentials of this type were found earlier,[20–22] but the associated electric field structures not recognized. Unlike those of "normal" solitons, hodograph plots of E against φ for supersolitons are characterized by the presence of inaccessible regions,[16,21] as we will illustrate below. Although, for conventional solitons, double layers are often found to represent the upper boundary of an existence region in parameter space, supersolitons typically occur for soliton speeds that exceed the double layer Mach number, M_{dl}.[21]

By establishing limiting conditions for the existence of supersolitons, one can systematically find regions in parameter space that may support supersolitons, rather than using a haphazard, trial-and-error approach. A lower bound arises from the existence of double layers. Other limits occur when the requirement of three local extrema in $S(\varphi)$ is breached through the merging of adjacent extrema, as illustrated in Fig. 2. This gives an example of a pseudopotential yielding a supersoliton (solid curve, with local extrema A, B, and C), lying between two pseudopotentials having standard soliton solutions. The latter arise from the coalescence of two local extrema, A and B (dotted-dashed curve) or B and C (dashed curve), respectively.

Previous examples of three-component plasmas that support appropriate pseudopotentials may be found in Refs. 21 and 22. The former considered ion-acoustic solitary waves in a plasma of two-temperature Boltzmann electrons and cold ions,[21] the latter, dust-acoustic solitons in a system of negative dust and two-temperature Boltzmann and nonthermal ("Cairns"[23]) positive ions.[22] We note that both of these models have wider applicability. Allowing for a sign reversal, Ref. 21 could describe dust-acoustic solitons in a plasma of two positive ion species and inertial negative dust, while Ref. 22 is also a model for Boltzmann and Cairns electrons, and inertial positive ions.

Both the above systems involve a single inertial species and two species that are effectively massless. To emphasize the wide range of three-component plasmas admitting supersolitons, we will consider here ion-acoustic solitons in a qualitatively different model with two *inertial* species of *opposite* polarity, comprising cold positive and negative ions, and nonthermal[23] electrons. Recently, Ref. 24 studied solitons in such a plasma but did not investigate supersolitons. Inter alia, heavy negative ions are relevant in the ionosphere[25] and cometary regions,[26] as well as the laboratory.[13]

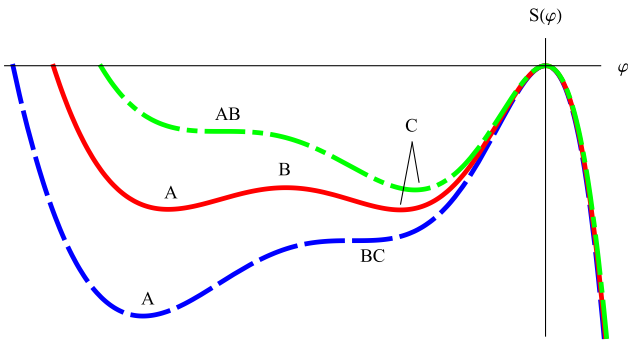

FIG. 2. Examples of pseudopotentials yielding a supersoliton (solid curve, with local extrema A, B and C), that lies between two standard solitons. These arise from the coalescence of two local extrema, A and B (dotted-dashed curve), and B and C (dashed curve), respectively.

Together with Refs. 21 and 22, and possibly other models, our investigations below show that supersolitons are not an artefact of exotic, complicated models, but refer to structures, whose electric field signatures should be observable in available or future space observations, where three-species plasmas are commonly found.

II. MODEL ANALYSIS

In our plasma model, the fraction of negative charge residing on the negative ions is $f = n_{n0}/n_0$ and on the electrons $1 - f = n_{e0}/n_0$, where n_0 is the positive ion density. For ease of presentation, the two ion species have been assumed singly charged, but that is not an essential restriction. The Cairns distribution,[23] commonly used in space plasma studies, models a Maxwellian with an enhanced nonthermal tail, which may be characterized by a parameter β.[27] Integration over velocity space yields the electron density,[28]

$$n_e(\varphi) = (1-f)(1 - \beta\varphi + \beta\varphi^2)\exp(\varphi), \tag{1}$$

where φ is normalized to T_e/e, with T_e the kinetic temperature (measured in energy units) the electrons would have in the absence of nonthermal effects, i.e., for $\beta = 0$.

The cold ions are described by the continuity and momentum equations, in variables[27] normalized to a typical speed, denoted by $C_{ia} = (T_e/m_p)^{1/2}$, and shielding length $(\varepsilon_0 T_e/n_0 e^2)^{1/2}$. Although we write the normalizing speed as C_{ia}, we emphasize that it is not the true acoustic speed in the present three-species plasma, but, as the ion-acoustic speed in a simple plasma composed of cold ions and Boltzmann electrons (i.e., for $f = \beta = 0$), it is a useful measure of speed. While in principle one is free to use any consistent set of scaling quantities to nondimensionalize the equations, we have chosen to leave parameters like f, β and μ explicitly outside the normalization, so as to be able to investigate the effect of variations in those parameters. Otherwise, some of the variations would be hidden in a changing normalization. The true ion-acoustic velocity for the plasma composition under consideration will be determined later, in Eq. (6).

Using the positive ion mass m_p in the normalization leads to a dimensionless mass ratio $\mu = m_n/m_p$. Should one wish to include arbitrary ion charge numbers, rather than singly ionized ions, μ could represent not just such a simple mass ratio, but the ratio of charge-to-mass ratios of the two ion species, together with a suitably-modified form for C_{ia}.

In a frame where the nonlinear structure is stationary $(\partial/\partial t = 0)$ and all variables tend to their undisturbed values at $x \to -\infty$, in particular $\varphi \to 0$, one can integrate the ion equations with respect to x and find normalized ion densities,

$$n_p = \left(1 - \frac{2\varphi}{M^2}\right)^{-\frac{1}{2}}, \qquad n_n = f\left(1 + \frac{2\varphi}{\mu M^2}\right)^{-\frac{1}{2}}. \tag{2}$$

These contain a kind of Mach number, $M = V/C_{ia}$, arising from ion inertial effects. It follows from these density expressions that limits on φ occur at $\varphi_{\ell n} = -\mu M^2/2$ (for the negative ions) and at $\varphi_{\ell p} = M^2/2$ (for the positive ions), beyond which the ion densities are no longer defined, as they reach infinite compression for $\varphi \to \varphi_{\ell n}$ or $\varphi_{\ell p}$. For $\mu > 1$ one notes that $\varphi_{\ell p} < |\varphi_{\ell n}|$. The larger existence range of the negative ion density suggests the possibility that enough wiggles might occur in $S(\varphi)$ for the existence of negative supersolitons. We shall consider such a case below.

The densities are substituted into Poisson's equation,

$$\frac{d^2\varphi}{dx^2} + n_p - n_n - n_e = 0. \tag{3}$$

After integration, this gives an energy-like integral,

$$\frac{1}{2}\left(\frac{d\varphi}{dx}\right)^2 + S(\varphi) = 0, \tag{4}$$

to be analyzed in terms of the Sagdeev pseudopotential

$$S(\varphi) = M^2\left(1 - \sqrt{1 - \frac{2\varphi}{M^2}}\right) + f\mu M^2\left(1 - \sqrt{1 + \frac{2\varphi}{\mu M^2}}\right) + (1-f)[1 + 3\beta - (1 + 3\beta - 3\beta\varphi + \beta\varphi^2)\exp(\varphi)]. \tag{5}$$

An important feature that follows immediately from Eq. (4) is that a local extremum in $S(\varphi)$ implies a local extremum in the electric field, which thus provides the link between the wiggles in $S(\varphi)$ and those in the bipolar structure of Fig. 1.

By assumption, $S(0) = S'(0) = 0$, but $S''(0) \leq 0$ is required for the origin to be a (local) unstable maximum, at least on one side. Here, primes denote derivatives of $S(\varphi)$ with respect to φ. The convexity condition, $S''(0) \leq 0$, yields

$$M^2 \geq M_s^2 = \frac{f + \mu}{\mu(1-\beta)(1-f)}, \tag{6}$$

where M_s is the *true* normalized acoustic speed in the three-species plasma. Thus, in physical terms, the nonlinear structures are (super)acoustic. Single nonzero roots of $S(\varphi)$ give positive or negative potential solitons, whereas for double roots φ changes from one value at $-\infty$ to another at $+\infty$, typical for potential kinks (double layers).

III. DISCUSSION

We now focus in a systematic way on where supersolitons may be found, by determining the limits in parameter space for their occurrence.

As we know from our work[20–22] and that of Ref. 16, supersoliton pseudopotentials include two local potential wells on one or the other side of $\varphi = 0$. We shall consider the case of negative potential supersolitons, and thus require at least three local extrema for $\varphi < 0$, as presented schematically by the solid curve in Fig. 2.

An important analytical tool in structuring the discussion is the generic property that $\partial S/\partial M < 0$,[29] which involves only the inertial species. Hence, for a fixed plasma composition and a chosen φ, one can obtain neighboring pseudopotentials by varying M, but these can never cross one another. Decreasing M increases the local maximum at B. A possible outcome of this process is that $S(\varphi)$ at B becomes zero and a double layer solution is obtained, for $M = M_{dl}$. A further decrease in M would push the maximum above zero, and the well lose its subsidiary extrema. Thus, the soliton speed at which a double layer solution occurs is clearly one of the lower limits on M for the existence of supersolitons.

Changing M might also lead to coalescence of two adjacent local extrema, either A and B or B and C. The two local "sub-wells" then merge into one, destroying the internal separatrix that is one of the characteristics of a supersoliton,[16] thus introducing other limits. In Fig. 2, we illustrate these possibilities for pseudopotentials with a supersoliton (solid curve) that lies between two standard solitons, when M is increased from the dotted-dashed (AB coalescence) to the dashed curve (BC coalescence).

We can now investigate some detailed examples, in order to extract the region in parameter space where supersolitons occur. This will be done for $\beta = 0.3$ and $\mu = 10$. It is well-known[27] that for $\beta > 4/7$ the Cairns distribution function is not single-humped, and thus potentially linearly unstable. Thus, given that the physically acceptable range is $0 \leq \beta < 4/7$, $\beta = 0.3$ is an appropriate intermediate choice. The mass ratio, $\mu = m_n/m_p = 10$ is an average value to cover several space applications. One can show (although not included here) that variations in μ over a rather wide range do not produce qualitative differences in regard to the existence and interpretation of the supersoliton phenomenon.

To start the quantitative discussion, we first pick $f = 0.3$, but hasten to add that this suitable choice will be seen not to be just based on a trial-and-error approach. In Fig. 3 four pseudopotentials are shown in the upper panel: at $M/M_s = 1.023$ (dotted curve) for a "normal" soliton, then at $M/M_s = 1.027$ (solid curve) for a double layer, and beyond that, e.g., at $M/M_s = 1.030$ (dashed curve) for a supersoliton and at $M/M_s = 1.035$ (dotted-dashed curve) for what is again a normal soliton, albeit a large one. These unusual values of M have been carefully chosen to illustrate neatly the supersoliton phenomenon. In much of the discussion and in the ordinate of Fig. 5 the quantity M/M_s appears. This is the true Mach number, since the normalizing velocity disappears from this ratio.

The top (dotted) curve represents a normal soliton, found here for a solitary wave speed that is a little smaller than M_{dl}. Increasing M/M_s to 1.027 yields the solid curve, which clearly represents a double layer at $M = M_{dl}$. A further small increase in M generates a Sagdeev pseudopotential with three subsidiary extrema, as shown by the dashed curve. This is an example of a supersoliton, with wiggles in $S(\varphi)$ which, as discussed below, will be reflected in associated wiggles in the electric field signature. Importantly, it is seen that the amplitudes exhibit a discrete jump as M is increased past M_{dl}, opening up a new range beyond the inaccessible root of the solid curve. This phenomenon was reported previously.[21] Hence, this shows that, for parameter values for which double layers are supported, supersolitons can only exist as part of a set of solitons for $M > M_{dl}$.

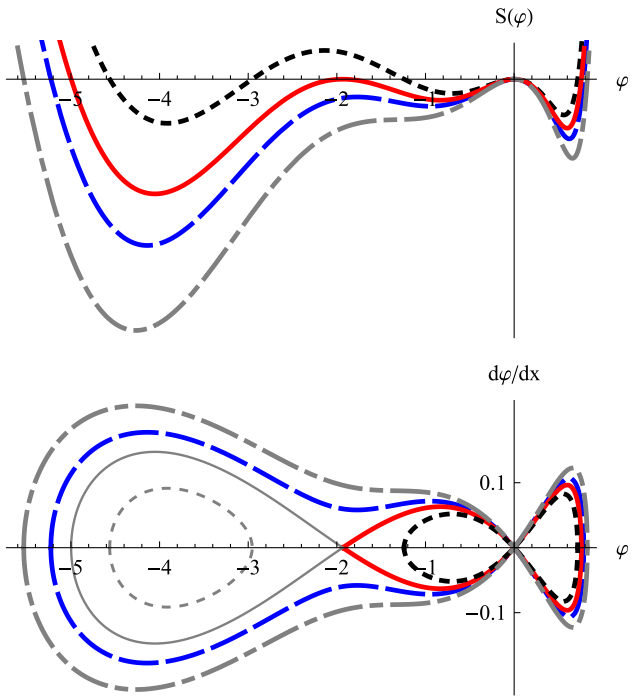

FIG. 3. *Upper panel:* Graphs of $S(\varphi)$ for $\beta = 0.3$, $\mu = 10$, $f = 0.3$ and $M/M_s = 1.023$ (dotted curve), $M/M_s = 1.027$ (solid curve), $M/M_s = 1.030$ (dashed curve) and $M/M_s = 1.035$ (dotted-dashed curve). *Lower panel:* Here the hodographs are presented, with the same curve coding. Thin dotted and solid curves in gray indicate ranges which are not accessible from the undisturbed conditions and thus physically irrelevant.

Other boundaries of the parameter range in which supersoliton may exist arise from the merging or disappearance of some of the local extrema. An example of this is seen in Fig. 3, where the dotted-dashed curve, for a slightly higher value of M, represents a normal soliton. As a result of a BC coalescence it has only a single well, and thus lies beyond the existence limit for supersolitons.

In addition to the negative roots discussed so far, the figure shows that there are also positive single roots, but these yield standard solitons only.

In Fig. 3, the lower panel presents the hodographs for these four values of M/M_s, with the same curve coding. The thinner parts of the dotted and solid curves in gray indicate ranges of the curves for the two lowest values of M, which are not accessible from the undisturbed conditions. A hodograph of this form is a prerequisite to encounter supersolitons.[16] The difference between the standard and the supersolitons is now very clear.

This difference is even more strongly accentuated when the *negative* supersoliton profile and its associated electric field are plotted, as shown in the lower panels of Fig. 1, which are not, in fact simply schematic, but were deduced from the dashed curve in Fig. 3. On the other hand, the upper panels in Fig. 1 illustrate the *positive* standard soliton associated with the positive potential part of the same dashed curve in Fig. 3. Note that our hodographs do not focus on the internal separatrices for a specific supersoliton, as in Ref. 16, but present the whole spread of pseudopotentials.

From Fig. 3 it becomes clear that when a double layer acts as lower limit for supersolitons, only a BC coalescence is possible and will act as the upper limit as M/M_s is increased, so that supersolitons occur for $M_{dl} < M < M_{BC}$ at given f. So the first question is: for which values of f are there double layers? One can easily check that both the double layer amplitude (in absolute value) and M_{dl} increase/decrease as f is increased/decreased, while the inaccessible third root decreases/increases. Lower limits in f are obtained when $M_{dl} = M_s$ which is found numerically to occur for $f = 0.239$, as $M < M_s$ does not yield solitons or double layers.

A negative double layer represents a double root, and as we see from the solid curve in Fig. 3, there are then three negative roots. If f is increased enough, the three negative roots will coalesce, as illustrated by the solid curve ($M/M_s = 1.046$) in Fig. 4. This triple root is found numerically to occur for $f = 0.332$, and these values of f and M signal the upper limits for which $S(\varphi)$ can have three negative roots. Together, this methodology provides a systematic determination of f for the existence of negative double layers. This indeed shows that our earlier choice of $f = 0.3$ for Fig. 2 is appropriate, as it clearly lies within the range in which double layers will exist and form the lower limit for the occurrence of supersolitons.

However, this is not the end of the supersoliton existence range, as, in the absence of double layers, other limits, such as the coalescence of local extrema, come into play. An example where such limits occur was used to generate Fig. 2, for which the value $f = 0.34$ was chosen. As we saw there, the lower and upper limits for the existence of supersolitons in such a plasma composition are governed by the AB and BC coalescences, respectively. Further increases in f narrow the range in M where supersolitons are encountered, until,

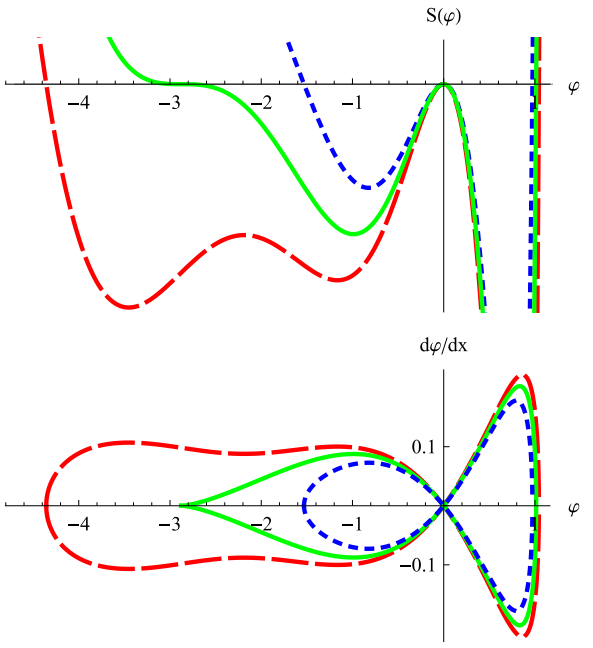

FIG. 4. *Upper panel:* Graphs of $S(\varphi)$ for $\beta = 0.3$, $\mu = 10$, $f = 0.332$ and $M/M_s = 1.040$ (dotted curve), $M/M_s = 1.046$ (solid curve) and $M/M_s = 1.051$ (dashed curve). The deep well on the positive side has been cut for graphical clarity. *Lower panel:* Here the hodographs are presented, with the same curve coding.

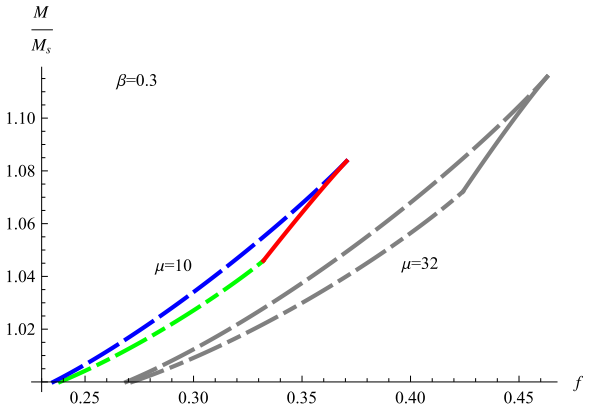

FIG. 5. Region where negative supersolitons can be found is above the dotted-dashed curve (occurrence of negative double layers) and the solid curve (*AB* coalescence), and below the dashed curve (*BC* coalescence). The lower corners occur at the acoustic speed, $M = M_s$, but at two different values of f. The upper corners are found at the triple root (signalling the end of the double layer range) and at the *ABC* coalescence. The gray graph is qualitatively similar but is drawn for $\mu = 32$.

finally, at $f = 0.371$ that possibility is lost, because then all three local extrema on the negative side merge into one, in what may be termed an *ABC* coalescence.

Hence, these considerations lead us in a methodical way to the existence diagram for supersolitons, in $\{f, M/M_s\}$ space, given in Fig. 5. The upper limit on M follows purely from encountering a *BC* coalescence of two extrema in the pseudopotential curve $S(\varphi)$. Indeed, an *AB* coalescence is not possible as long as there are double layers, and, as Fig. 2 shows, $M_{AB} \leq M_{BC}$.

There are, however, three possible lower limits for supersolitons in our case study with $\beta = 0.3$ and $\mu = 10$. First, there is a tiny range at the true acoustic speed, $M = M_s$ (between $f = 0.235$ and 0.239), before negative double layers can occur. Next, the dotted-dashed double layer curve is the limit, up to the triple root at $f = 0.332$. The last stretch is an *AB*-type coalescence, up to $f = 0.371$, shown by the solid curve. Again, we stress that these limits can be determined in a systematic way: double layers by solving $S(\varphi) = S'(\varphi) = 0$ for common values of φ, M, for a given composition, and similarly, for the coalescence of negative extrema, by solving $S'(\varphi) = S''(\varphi) = 0$. For the plasma composition under consideration, with $\beta = 0.3$ and $\mu = 10$, there are, of course, no positive supersolitons.

The gray graph in Fig. 5 represents the existence domain for a plasma involving O_2^- [25] and illustrates that the change of mass ratio μ from the indicative value of 10 to $\mu = 32$ does not have a qualitative effect but merely pushes the existence domains to higher values of f and M.

IV. SUMMARY AND OUTLOOK

To conclude, we have considered the existence of "supersoliton" structures in plasmas from first principles. We have shown that supersolitons are not an artefact of rather exceptional or complicated plasma models, but that they can exist in various three-component plasmas. Moreover, the existence regime in parameter space is detailed in a methodical fashion, by determining the specific limiting factors. Although we have dealt here with $\beta = 0.3$ and $\mu = 10$, we have also carried out computations for other values of these parameters. Considering a wide range of plasma configurational parameters, we have shown that supersolitons may occur in specific regions ("islands"), delimited by boundaries which can be found numerically in a systematic manner.

Based on our findings, it appears that electrostatic supersolitons cannot exist in two-species plasmas, at least not for the traditional fluid models of cool and hot species. Finally, it is proposed that the telltale electric field signatures of supersolitons should be sought in available or future space or laboratory observations in three-species plasmas. One example can be seen in Cluster data,[18] where their Figure 1(b) clearly shows a supersoliton electric field wedged between two regular bipolar structures. In the laboratory, these should appear as "distorted" bipolar electric field forms, which may be resolved, e.g., via proton imaging,[14] among other techniques. The subtlety in the latter case would be in the preparation of the multi-ion plasmas, along with technical challenges, e.g., in probing and diagnostics, that might make detecting supersolitons feasible, but not an easy task.[30] We see this as an intriguing direction of future research.

ACKNOWLEDGMENTS

M.A.H. thanks the South African National Research Foundation for support. I.K. warmly acknowledges support from the UK Engineering and Physical Sciences Research Council (EPSRC) via Grant No. EP/I031766/1.

[1]T. Dauxois and M. Peyrard, *Physics of Solitons* (Cambridge University, Cambridge, U.K., 2005).
[2]D. J. Korteweg and G. De Vries, Philos. Mag. **39**, 422 (1895).
[3]N. J. Zabusky and M. D. Kruskal, Phys. Rev. Lett. **15**, 240 (1965).
[4]J. E. Allen, Phys. Scr. **57**, 436 (1998).
[5]R. Z. Sagdeev, *Reviews of Plasma Physics*, edited by M. A. Leontovich (Consultants Bureau, New York, 1966), Vol. 4, p. 23.
[6]J. F. McKenzie, Phys. Plasmas **9**, 800 (2002).
[7]F. Verheest, T. Cattaert, G. S. Lakhina and S. V. Singh, J. Plasma Phys. **70**, 237 (2004).
[8]M. Temerin, K. Cerny, W. Lotko, and F. S. Mozer, Phys. Rev. Lett. **48**, 1175 (1982).
[9]R. Boström, G. Gustafsson, B. Holback, G. Holmgren, H. Koskinen, and P. Kintner, Phys. Rev. Lett. **61**, 82 (1988).
[10]R. E. Ergun, L. Andersson, J. Tao *et al.*, Phys. Rev. Lett. **102**, 155002 (2009).
[11]N. Dubouloz, R. Pottelette, M. Malingre, and R. A. Treumann, Geophys. Res. Lett. **18**, 155, doi:10.1029/90GL02677 (1991).
[12]R. Pottelette, R. E. Ergun, R. A. Treumann, M. Berthomier, C. W. Carlson, J.P. McFadden, and I. Roth, Geophys. Res. Lett. **26**, 2629, doi:10.1029/1999GL900462 (1999).
[13]G. O. Ludwig, J. L. Ferreira, and Y. Nakamura, Phys. Rev. Lett. **52**, 275 (1984).
[14]L. Romagnani, S. V. Bulanov, M. Borghesi, P. Audebert, J. C. Gauthier, K. Löwenbrück, A. J. Mackinnon, P. Patel, G. Pretzler, T. Toncian, and O. Willi, Phys. Rev. Lett. **101**, 025004 (2008).
[15]B. Lefebvre, L.-J. Chen, W. Gekelman, P. Kintner, J. Pickett, P. Pribyl, S. Vincena, F. Chiang, and J. Judy, Phys. Rev. Lett. **105**, 115001 (2010).
[16]A. E. Dubinov and D. Yu. Kolotkov, IEEE Trans. Plasma Sci. **40**, 1429 (2012).
[17]A. E. Dubinov and D. Yu. Kolotkov, High Energy Chem. **46**, 349 (2012).
[18]J. S. Pickett, L.-J. Chen, S. W. Kahler, O. Santolík, D. A. Gurnett, B. T. Tsurutani, and A. Balogh, Ann. Geophys. **22**, 2515 (2004).
[19]R. E. Ergun, C. W. Carlson, J. P. McFadden, F. S. Mozer, L. Muschietti, I. Roth, and R. J. Strangeway, Phys. Rev. Lett. **81**, 826 (1998).

[20]F. Verheest, Phys. Plasmas **16**, 013704 (2009).
[21]T. K. Baluku, M. A. Hellberg, and F. Verheest, Europhys. Lett. **91**, 15001 (2010).
[22]F. Verheest, Phys. Plasmas **18**, 083701 (2011).
[23]R. A. Cairns, A. A. Mamun, R. Bingham, R. Boström, R. O. Dendy, C. M. C. Nairn, and P. K. Shukla, Geophys. Res. Lett. **22**, 2709, doi:10.1029/95GL02781 (1995).
[24]R. Sabry, W. M. Moslem, and P. K. Shukla, Phys. Plasmas **16**, 032302 (2009).
[25]J. K. Hargreaves, *The Upper Atmosphere and Solar-Terrestrial Relations*, (Van Nostrand Reinhold, Wokingham, Berks, England, 1979), p. 76.
[26]P. Chaizy, H. Rème, J. A. Sauvaud, C. d'Uston, R. P. Lin, D. E. Larson, D. L. Mitchell, K. A. Anderson, C. W. Carlson, A. Korth, and D. A. Mendis, Nature **349**, 393 (1991).
[27]F. Verheest and S. R. Pillay, Phys. Plasmas **15**, 013703 (2008).
[28]F. Verheest and M. A. Hellberg, Phys. Plasmas **17**, 102312 (2010).
[29]F. Verheest, Phys. Plasmas **17**, 062302 (2010).
[30]M. Borghesi, private communication (2012).